*European Journal of Organic Chemistry*

WILEY VCH

EurJOC
European Journal of Organic Chemistry

Chemistry Europe
European Chemical Societies Publishing

RESEARCH ARTICLE OPEN ACCESS

# Modular Synthesis of Dihydropyranones through Cyclization and Organometallic Functionalization

Markéta Fuksová[1] | Kristýna Hrubá[2] | Adam Horák[2] | Corinne De Dobbeleer[3] | Raphaël Robiette[4] | Jiří Pospíšil[1,2,3]

[1]Department of Chemical Biology, Palacky University Olomouc, Olomouc, Czech Republic | [2]Department of Organic Chemistry, Palacky University Olomouc, Olomouc, Czech Republic | [3]Laboratory of Growth Regulators, Palacky University & Institute of Experimental Botany AS CR, Olomouc, Czech Republic | [4]Institute of Condensed Matter and Nanosciences, Université Catholique de Louvain, Louvain-la-Neuve, Belgium

**Correspondence:** Jiří Pospíšil (j.pospisil@upol.cz)

**Received:** 24 August 2025 | **Revised:** 28 October 2025 | **Accepted:** 29 October 2025

**Funding:** Internal Grant Agency of Palacky University, Grant/Award Numbers: IGA_PrF_2025_013 IGA_PrF_2025_014 IGA_PrF_2025_019; European Regional Development Fund-Project "TowArds Next GENeration Crops", Grant/Award Number: CZ.02.01.01/00/22_008/0004581; European Union; European Regional Development Fund-Project "SMART Plant Biotechnology for Sustainable Agriculture", Grant/Award Number: CZ.02.01.01/00/23_020/0008497; Fonds de la Recherche Scientifique-FNRS (F.R.S.-FNRS), Grant/Award Number: 2.5020.11

**Keywords:** base-promoted cyclization | deuterium labeling | dihydropyranone synthesis | natural product synthesis | organometallic addition

## ABSTRACT

Dihydropyranones are key structural motifs in biologically active polyketides. We report a reproducible and scalable method for synthesizing 3-methoxy-4,5-dihydropyran-2-ones (MeO-DHP-2-ones) via base-promoted cyclization of hydroxy alkynes. Mechanistic and computational studies revealed that water content and reaction time critically influence lactonization efficiency. Two optimized protocols – using potassium carbonate ($K_2CO_3$) or in situ generated sodium methoxide (MeONa) – enabled consistent yields across multiple substrates. Cyclization in deuterated methanol provided deuterium-enriched DHP-2-one scaffolds with high isotopic incorporation, valuable for mechanistic and medicinal applications. The transformation of DHP-2-ones into 4,5-dihydropyran-4-ones (DHP-4-ones) was achieved via organometallic addition followed by a tailored workup involving aqueous hydrochloric acid and boron trifluoride diethyl etherate ($BF_3{\cdot}OEt_2$). This protocol proved robust and scalable, compatible with both organolithium and organomagnesium reagents, although the latter afforded lower yields. Mechanistic analysis highlighted key steps including hemiacetal formation, oxonium activation, and controlled hydrolysis. The methodology enables multigram-scale preparation of both DHP-2-one and DHP-4-one scaffolds and provides a streamlined route toward spiroacetal precursors.

## 1 | Introduction

Polyketides represent a major class of natural products characterized by remarkable structural diversity originating from the simple building block – acetic acid [1, 2]. Their varied architectures – including polyethers, polyenes, polyphenols, macrolides, enediynes, and numerous heterocyclic scaffolds – make them invaluable as therapeutic agents and molecular probes [3–5]. Among these diverse structures, dihydropyranones (Figure 1A) have emerged as key components in terms of biological activity [3, 4, 6]. It has been demonstrated that even small changes within the dihydropyranone core can substantially alter their biological activity [2]. Therefore, we hypothesized that simple late-stage transformations of various dihydropyranone cores could facilitate the identification of novel biological activities within this compound family.

To validate our approach, we focused on three related motifs: 3-methoxy-4,5-dihydropyran-2-one (**1**), 4,5-dihydropyran-4-one (**2**), and spiroacetal (**3**), all central to our ongoing research in

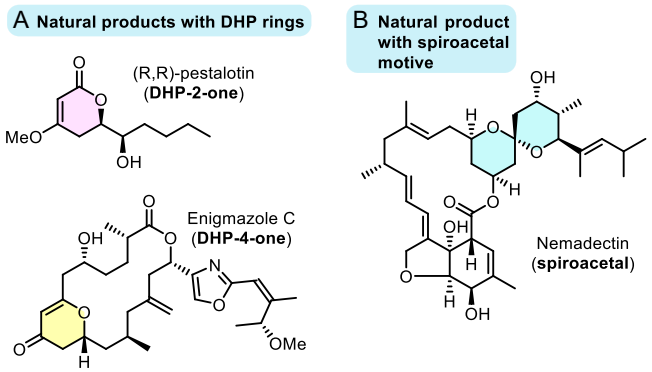


**FIGURE 1** | (A) Selected examples of natural products containing dihydropyran-2-one (**DHP-2-one**) and dihydropyran-4-on (**DHP-4-one**) structural motives within the structure. (B) An example of spiroacetal subunit-containing natural product.

anthelmintic compound development (Figure 1B). Given their structural similarities, we anticipated that these scaffolds could be readily interconverted, enabling a streamlined strategy in which readily available lactone heterocycles **1** (*DHP-2-one* core) are transformed into *DHP-4-one* scaffolds **2**, and subsequently into *spiroacetal* **3** (Scheme 1A). A comprehensive literature review indicated that this approach is potentially viable. It was found out that while synthetic routes to MeO-DHP-2-one **1** are well established (Scheme 1B) [7–12], only a single precedent has been reported for its conversion into the DHP-4-one **2** framework (Scheme 1C) [13]. In contrast, the subsequent transformation of DHP-4-one into *spiroacetal* **3** is again well documented (Scheme 1D) [14–18].

As mentioned above, MeO-DHP-2-one (**1**) scaffolds are prepared via a hetero-Diels–Alder reaction [7, 8] or by a Mukaiyama aldol reaction followed by cyclization promoted by a base or a Lewis acid [9–12] (Scheme 1B). We were, however, drawn to a less-explored approach based on the addition of methanolate to an activated alkyne (Scheme 2). This method is particularly attractive because the alkyne precursor is available in homochiral form from the corresponding epoxide. Surprisingly, despite the prevalence of the unsubstituted C5 MeO-DHP-2-one motif in natural polyketides [2, 3, 5, 19], this methanolate – alkyne route has been reported only 10 times – a scarcity we later on attributed to reproducibility issues in the cyclization step [20–28].

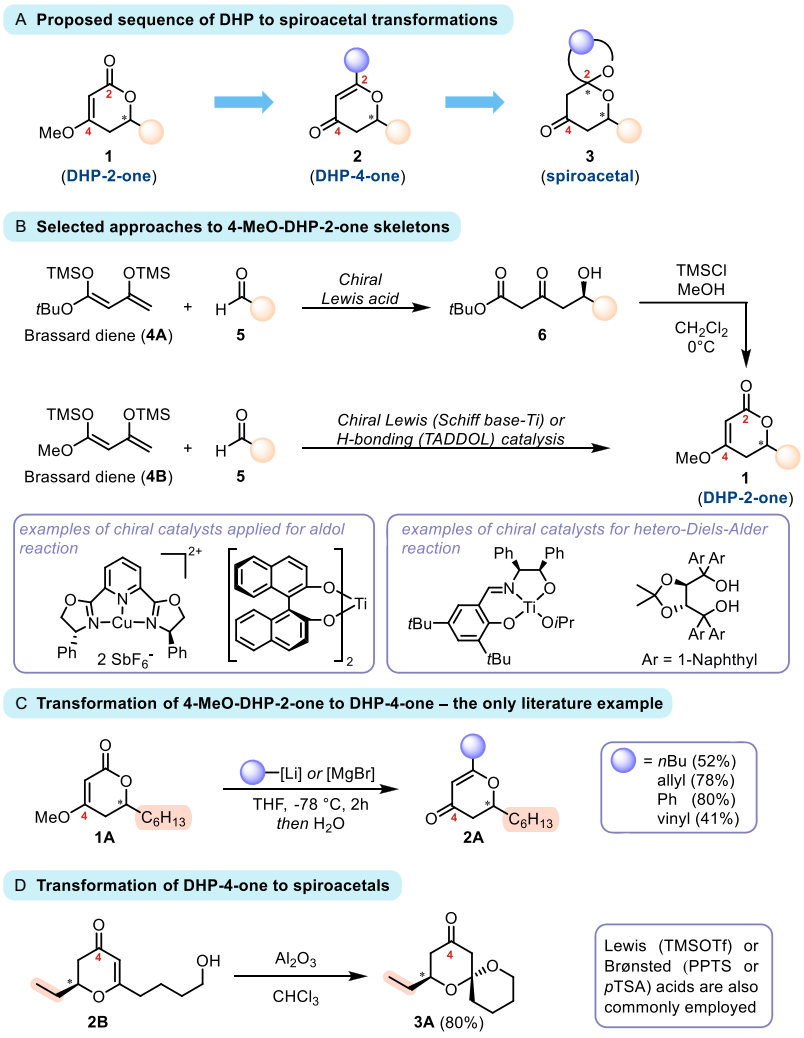


**SCHEME 1** | (A) Proposed strategy enabling the efficient transformation of DHP-2-one (**1**) scaffolds into DHP-4-one (**2**) and spiroacetal (**3**) motifs. (B) Established synthetic approaches to 4-MeO-DHP-2-one (**1**) heterocycles, including Brassard diene-based methods utilizing Mukaiyama aldol/cyclization sequences and the hetero-Diels–Alder strategy. (C) The only reported example of DHP-2-one (**1**) conversion into a DHP-4-one (**2**) heterocycle. (D) Spiroacetal (**3**) synthesis using the DHP-4-one framework as the starting material.

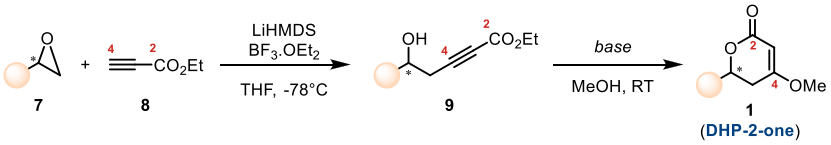


**SCHEME 2** | Underdeveloped approach to DHP-2-one scaffolds (**1**) based on the epoxide **7** opening and base-triggered Michael-addition/cyclization sequence.

In this contribution, we detail the challenges encountered during the synthesis of our model MeO-DHP-2-one (**1**) scaffolds. Our comprehensive mechanistic study, which combines experimental and theoretical approaches, reveals that reaction time and the presence of water are critical factors affecting lactonization efficiency. Furthermore, we demonstrate that these scaffolds can be readily converted into the corresponding DHP-4-one (**2**) heterocycles, thereby paving the way for subsequent spiroacetal (**1**) formation.

## 2 | Results and Discussion

Our interest in the base-promoted cyclization of hydroxy alkyne **9** was sparked by challenges encountered during the scale-up of the lactonization of (*S*)-**9a** – a precursor to DHP-2-one (*R*)-**1a** and a key intermediate in the synthesis of the spiroacetal structural motive (Scheme 3). Notably, similar difficulties arose in two other projects within our group that employed the same intermediates and transformation sequences.

Given the reported tendency of primary sodium alkoxides to decompose in the solid state [29], we first set out to evaluate the influence of base selection on reaction yields (Table S1). A range of inorganic and organic bases was tested; however, none led to an improvement in yield under comparable reaction conditions. At that point, an NMR study of the (*S*)-**9a** cyclization promoted by $K_2CO_3$ was carried out (see Supporting Information).

Combined evidence from $^1$H NMR spectroscopy [30] and preparative reactions conducted in methanol-*d* and methanol-$d_4$ (Scheme 4A) revealed that the cyclization process involves not only the incorporation of a $d_3$-methoxy group and deuterium at the C2 position of the newly formed lactone ring, but also a near-quantitative replacement of hydrogen atoms at the C5 position with deuterium (deuterium incorporation >93% in all cases).

Additionally, the lactone (*R*)-**1a** (Scheme S2A) was found to be unstable under the reaction conditions, undergoing gradual degradation over time. Even under optimized conditions ($K_2CO_3$, 5 equiv, 1 h), scaling up the reaction proved nonreproducible, regardless of the substrate used (Scheme S2B). This prompted an investigation into the role of residual water in methanol, which was identified as a key factor influencing cyclization yield (Scheme 4B).

Various methanol drying protocols were evaluated [31], and the highest yields were obtained when methanol containing approximately 12 ppm of water was used. This was achieved by sequential treatment with 3 Å molecular sieves (20% m/V) followed by Mg/$I_2$. Although reproducible, this protocol was time-consuming. To simplify the procedure, we adopted a modified approach using predried methanol (treated with 3 Å molecular sieves, 20% m/V), followed by in situ generation of sodium methoxide via reaction with sodium metal (Scheme 4C). Under these conditions, lactonization proceeded over a slightly extended reaction time (2 h instead of 1 h) and with somewhat lower yield, likely due to the reduced nucleophilicity of sodium methoxide compared to potassium methoxide. Nevertheless, the reaction was reproducible across different scales. The lower yield is presumably attributable to degradation of the product or reactive intermediates.

Computational analysis of the reaction pathway for the seemingly straightforward conversion of alcohol (*S*)-**9a** to lactone (*R*)-**1a** revealed a complex network of equilibria (Scheme 4D; only the direct pathway is shown; full mechanism available in Supporting Information). The data indicate that nucleophilic addition of methoxide to the alkyne moiety is the rate-determining step.

Based on the combined experimental and computational data, a reliable reaction mechanism was proposed (Scheme 5). Initially, transesterification of ethyl ester (*S*)-**9a** to methyl ester (*S*)-**Me-9a** occurs. Methoxide, acting as both base and nucleophile, may either deprotonate the C5 position of (*S*)-**Me-9a** to form

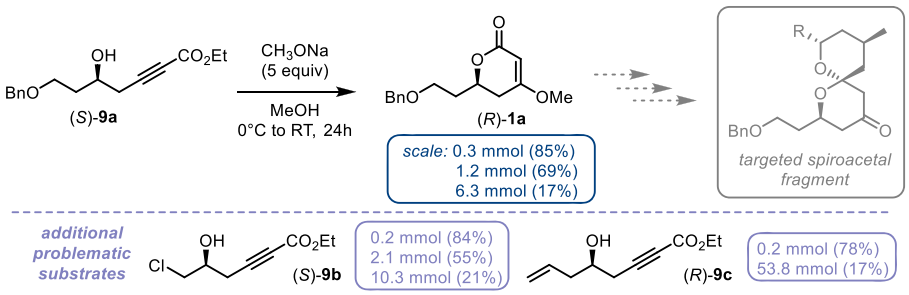


**SCHEME 3** | Problems encountered during the scale-up of the lactonization reactions of alkynes **9**.

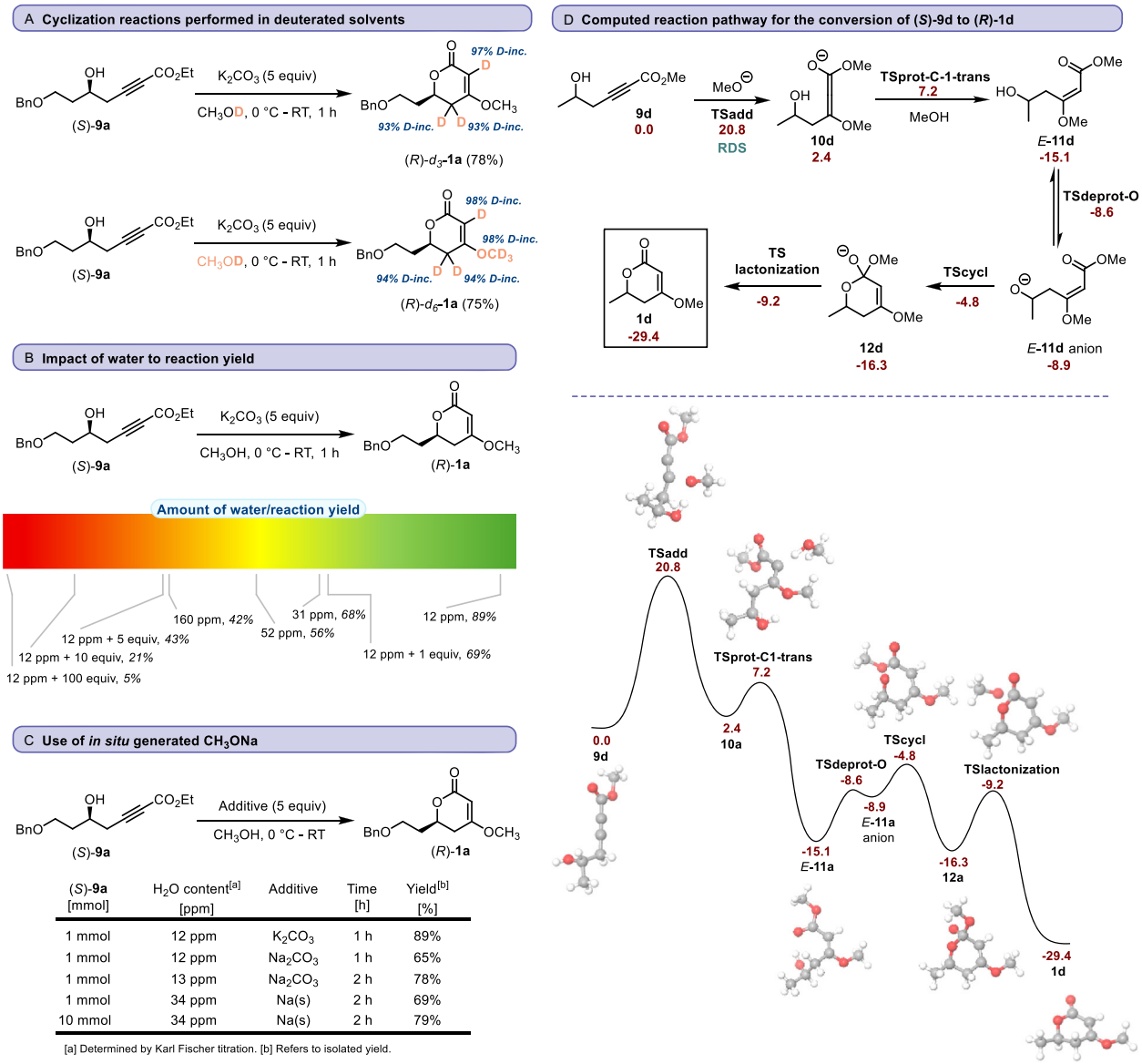


| (S)-9a [mmol] | $H_2O$ content[a] [ppm] | Additive | Time [h] | Yield[b] [%] |
|---|---|---|---|---|
| 1 mmol | 12 ppm | $K_2CO_3$ | 1 h | 89% |
| 1 mmol | 12 ppm | $Na_2CO_3$ | 1 h | 65% |
| 1 mmol | 13 ppm | $Na_2CO_3$ | 2 h | 78% |
| 1 mmol | 34 ppm | Na(s) | 2 h | 69% |
| 10 mmol | 34 ppm | Na(s) | 2 h | 79% |

[a] Determined by Karl Fischer titration. [b] Refers to isolated yield.

**SCHEME 4** | (A) Cyclization of (*S*)-**9a** to lactone (*R*)-**1a** performed in methanol-$d_1$ and methanol-$d_4$. (B) Impact of water content on reaction yield – selected examples. The correlation between added water and the isolated yield of (*R*)-**1a** is showed. Water content in methanol was quantified using Karl Fischer coulometric titration [33]. For more details see Table S2. (C) Use of in situ generated $CH_3ONa$ as a $K_2CO_3$ equivalent. (D) Computational study of reaction pathways was carried out at the LCCSD/cc-pVTZ(MeOH)//B3LYP-D3/6-31+G(d)(MeOH) level using the simplified model compound **9d.** Free energies are reported in kcal.mol$^{-1}$ relative to reactants. Only the direct reaction pathway is depicted. For details on side reactions and equilibrium processes, see Supporting Information. RDS = rate-determining step.

intermediate **13a** (a reversible process under reaction conditions), or add across the alkyne to yield intermediate **10a**. The formation of **13a** is unlikely, as no C5-deuterated alcohol (*S*)-**Me-9a** was detected in reactions conducted in methanol-$d_4$ [30].

Intermediate **10a** undergoes protonation to form two possible species: *E*-**11a** and *Z*-**11a** [32]. *E*-**11a** is suitably arranged for lactonization, which follows alcohol deprotonation at C6, and readily yields lactone (*R*)-**1a**. In contrast, *Z*-**11a** cannot cyclize due to unfavorable spatial arrangement of substituents. Its isomerization via intermediate *Z*, *E*-**14a** to *E*-**11a** is therefore essential. The formation of intermediates **14a** is likely responsible for the nearly quantitative deuterium incorporation at C5 in lactone (*R*)-**1a**, suggesting that isomerization from **11a** to **14a** is a rapid process.

Finally, computational data suggest that lactone (*R*)-**1a** can be readily converted under reaction conditions to the anionic species **15a** [30]. Although **15a** was not detected experimentally (see NMR studies [30]), its formation is believed to contribute to the degradation of the target lactone under basic conditions. Experimental data further indicate that the presence of water accelerates this degradation.

Having clarified the reaction mechanism and addressed reproducibility issues, two sets of optimized reaction conditions were established. All five key substrates **9a–c,e,f** were then tested under both protocols (Scheme 6). In all cases, reproducible yields of the corresponding lactones [34] were obtained. Notably, lactonization promoted by $K_2CO_3$ consistently yielded slightly higher

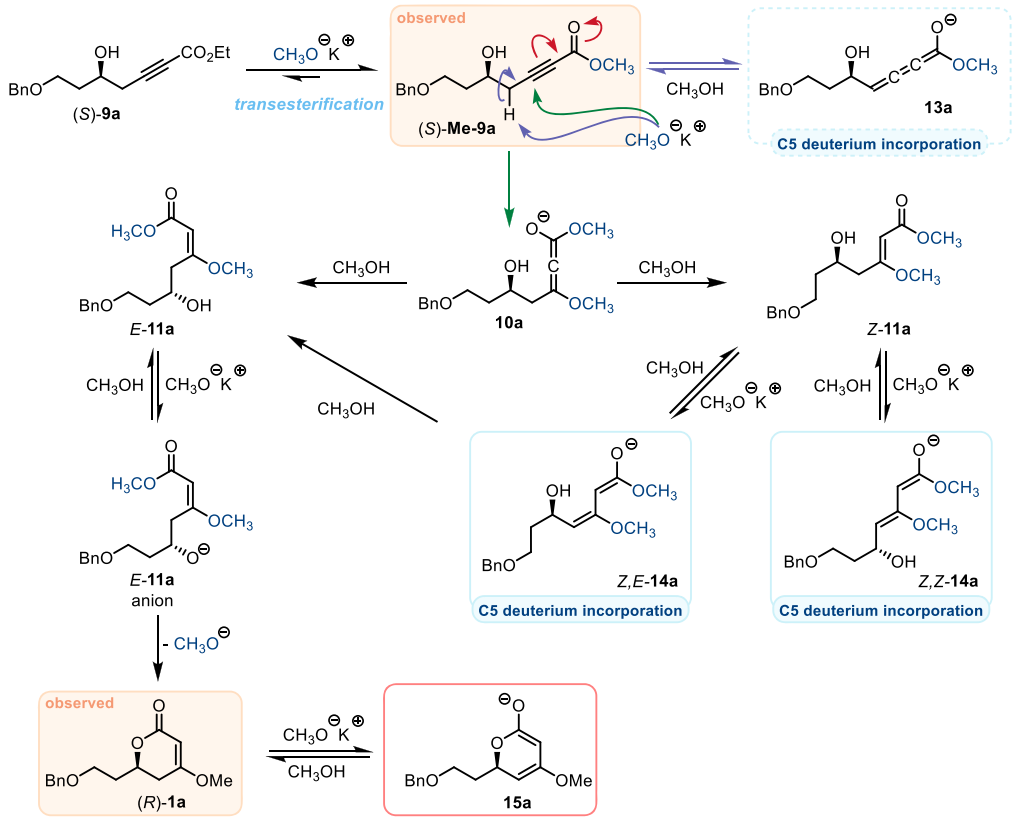


**SCHEME 5** | Proposed reaction mechanism of the alcohol (*S*)-**9a** transformation to lactone (*R*)-**1a**.

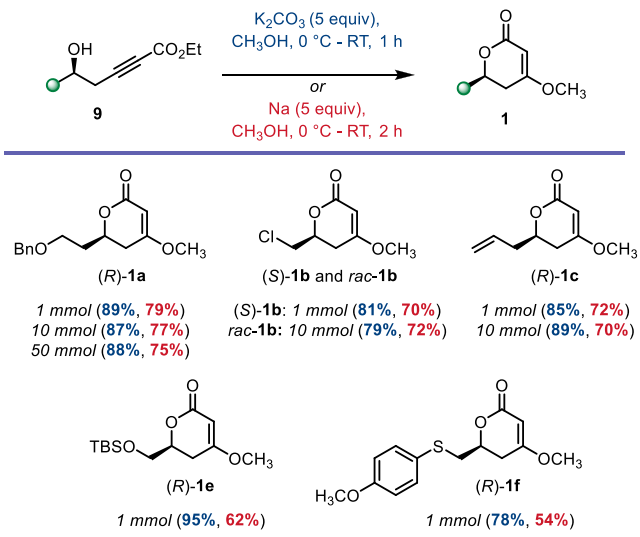


**SCHEME 6** | Comparison of cyclization conditions for the transformation of alcohols **9a–c** to lactones **1a–c**. Reaction yields are shown for two optimized protocols: $K_2CO_3$-promoted cyclization (blue) and in situ generation of MeONa (red).

amounts of lactones **1** than the conditions based on in situ generation of MeONa.

With a reliable route to lactone **1** established, we next investigated its transformation into DHP-4-one **2**. As previously noted, our strategy was inspired by the sole publication of Winkler and Oh [13], which described the addition of organolithium and organomagnesium reagents to the carbonyl group of lactone **1**. Upon evaluating their reported protocol, we obtained the desired DHP-4-one **2a** in only 32% yield (Scheme 7A).

Further investigation into the transformation of DHP-2-one **1** to the DHP-4-one **2** skeleton (Scheme 7B) revealed that the key challenge lies in converting adduct **16** into the final product. Mechanistically, this transformation proceeds through a sequence of critical events: initially, adduct **16** undergoes protonation to generate the free hemiacetal intermediate **17**. This intermediate then requires activation of its hydroxy group, facilitating the formation of the oxonium species **19**. Finally, hydrolysis of the resulting intermediate **19B** leads to the formation of the desired enone **2**. Each of these steps is essential for the successful enol ether hydrolysis and enone formation.

To accommodate these mechanistic requirements, a tailored reaction workup was designed to combine aqueous acidic conditions – necessary for both protonation and hydrolysis – with conditions conducive to oxonium formation (Table S3). Gratifyingly, sequential treatment with 1.0 M aqueous HCl followed by $BF_3{\cdot}OEt_2$ proved effective in accomplishing the transformation (Scheme 7C). The optimized workup protocol demonstrated robustness, reproducibility, and scalability, and enabled the preparation of DHP-4-ones **2** from the DHP-2-one **1** skeleton on a multigram scale (Scheme 7C). As expected, the alkyl chlorine-containing substrate **1b** was incompatible with these conditions. Both organolithium and organomagnesium reagents can be employed in this protocol; however, the latter typically affords the desired products in lower yields – an observation that aligns with the original report by Winkler and Oh [13].

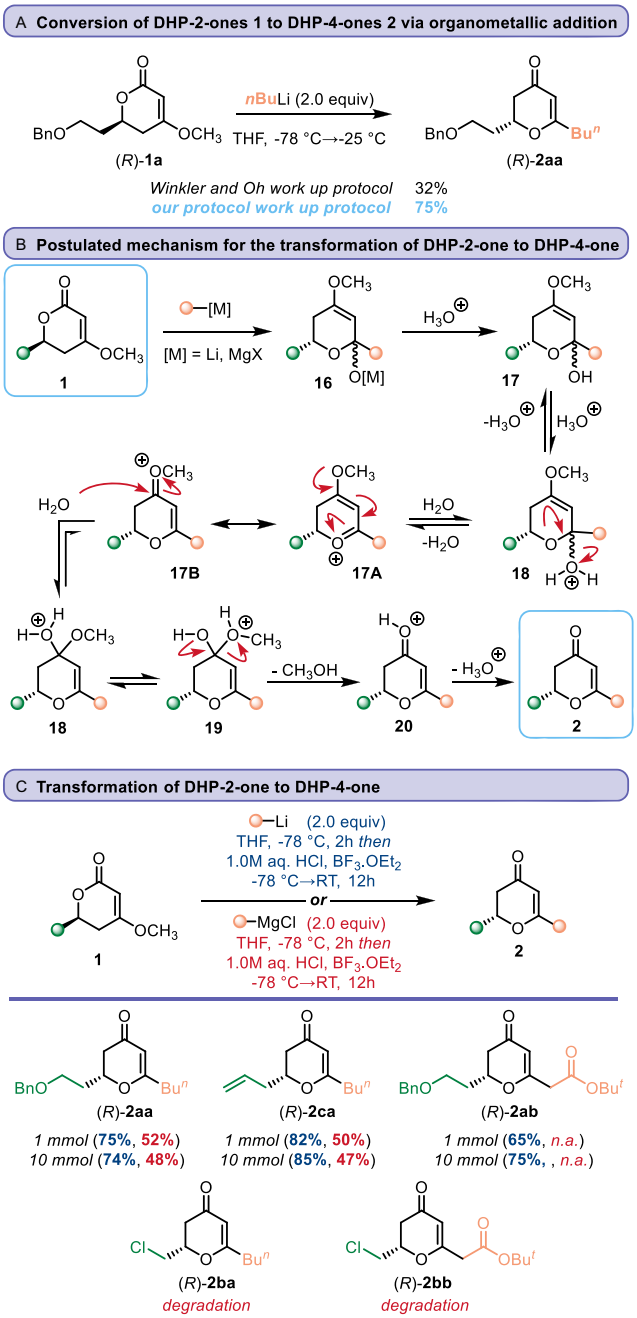


**SCHEME 7** | Transformation of DHP-2-one **1** to DHP-4-one **2**. (A) Comparison of workup protocols from the original publication [13] (Winkler and Oh) with our newly developed method employing 1.0 M aqueous hydrochloric acid (HCl) and $BF_3{\cdot}OEt_2$, highlighting their impact on the reaction yield. (B) Proposed reaction mechanism for the conversion of DHP-2-one **1** to DHP-4-one **2**. (C) Application of optimized protocols for organolithium (blue) and organomagnesium (red) reagents to substrates **1a–c** and the influence of reaction scale on isolated yields. $Bu^n$ = *n*-butyl; $Bu^t$ = *tert*-butyl; n.a. = not attempted.

## 3 | Conclusion

We have developed a robust, reproducible, and scalable methodology for the synthesis of MeO-DHP-2-one scaffolds via base-promoted cyclization of hydroxy alkynes. Through a combination of experimental and computational studies, we identified water content and reaction time as critical parameters governing lactonization efficiency and reproducibility. These insights enabled the establishment of two optimized protocols – using either $K_2CO_3$ or in situ generated MeONa – that consistently delivered high yields across multiple substrates and scales. Importantly, we showed that performing the cyclization in deuterated methanol enables the synthesis of deuterium-enriched DHP-2-one skeletons with high levels of isotopic incorporation at well-defined positions. This feature enhances the value of these compounds for mechanistic investigations and potential applications in medicinal chemistry. We further demonstrated the successful transformation of DHP-2-one scaffolds into DHP-4-one heterocycles using a tailored workup protocol involving sequential treatment with aqueous HCl and $BF_3{\cdot}OEt_2$. This protocol proved scalable and compatible with both organolithium and organomagnesium reagents, although the latter afforded lower yields. The choice of the workup protocol clearly highlighted the importance of hemiacetal formation, oxonium activation, and controlled hydrolysis steps depicted in the generally accepted reaction mechanism.

Overall, the methodology enables multigram-scale preparation of both DHP-2-ones and DHP-4-ones and lays a solid foundation for subsequent spiroacetal formation. We are currently applying this strategy in the synthesis of complex natural products, underscoring its practical utility and broad applicability in synthetic organic chemistry.


### Acknowledgments

The authors gratefully acknowledge Tomáš Pospíšil, Ph.D. (Department of Chemical Biology, Palacký University) for his assistance with NMR experiments, Dr. Zhang Chao (Department of Chemical Biology, Palacký University) for conducting HRMS analyses, and Assoc. Prof. Ivan Němec, Ph.D. (Department of Inorganic Chemistry, Palacký University) for performing X-ray crystallographic studies. M.F., K.H., and C.D.D. are grateful to Internal Grant Agency of Palacky University (IGA_PrF_2025_013, IGA_PrF_2025_014, and IGA_PrF_2025_019) for the financial support. M.F. is grateful to support provided by the European Regional Development Fund-Project "TowArds Next GENeration Crops" (No. CZ.02.01.01/00/22_008/0004581), co-funded by the European Union. J.P. is grateful to support provided by the European Regional Development Fund-Project "SMART Plant Biotechnology for Sustainable Agriculture" (No. CZ.02.01.01/00/23_020/0008497), co-funded by the European Union. Computational resources have been provided by the supercomputing facilities of the Université catholique de Louvain (CISM/UCL) and the Consortium des équipements de Calcul Intensif en Fédération Wallonie Bruxelles (CéCI) funded by the Fonds de la Recherche Scientifique-FNRS (F.R.S.-FNRS) under convention 2.5020.11 and by the Walloon Region. R.R. is a senior researcher of the F.R.S.-FNRS.

Open access publishing facilitated by Univerzita Palackeho v Olomouci, as part of the Wiley - CzechELib agreement.


### Conflicts of Interest

The authors declare no conflicts of interest.

### Data Availability Statement

The data that support the findings of this study are available in the supplementary material of this article and the data that support the findings of this study related to chemical synthesis and NMR studies part are openly available in Zenodo at 10.5281/zenodo.16936825.

## References


1. C. Hertweck, "The Biosynthetic Logic of Polyketide Diversity," *Angewandte Chemie, International Edition* 48 (2009): 4688–4716.

2. X. Di, P. Li, Y. Xiahou, H. Wei, S. Zhi, and L. Liu, "Recent Advances in Discovery, Structure, Bioactivity, and Biosynthesis of Trans -AT Polyketides," *Journal of Agricultural and Food Chemistry* 72 (2024): 21318–21343.

3. L. Wang, H. Lu, and Y. Jiang, "Natural Polyketides Act as Promising Antifungal Agents," *Biomolecules* 13 (2023): 1572.

4. D. J. Newman and G. M. Cragg, "Natural Products as Sources of New Drugs from 1981 to 2014," *Journal of Natural Products* 79 (2016): 629–661.

5. I. Paterson and N. Y. S. Lam, "Challenges and Discoveries in the Total Synthesis of Complex Polyketide Natural Products," *Journal of Antibiotics* 71 (2018): 215–233.

6. S. K. Sartori, M. A. N. Diaz, and G. Diaz-Muñoz, "Lactones: Classification, Synthesis, Biological Activities, and Industrial Applications," *Tetrahedron* 84 (2021): 132001.

7. Q. Fan, L. Lin, J. Liu, Y. Huang, X. Feng, and G. Zhang, "Highly Enantioselective Hetero-Diels - Alder Reaction of Brassard Diene with Aromatic Aldehydes," *Organic Letters* 6 (2004): 2185–2188.

8. H. Du, D. Zhao, and K. Ding, "Enantioselective Catalysis of the Hetero-Diels-Alder Reaction between Brassard's Diene and Aldehydes by Hydrogen-Bonding Activation: A One-Step Synthesis of (S)-(+)-Dihydrokawain," *Chemistry - A European Journal*10 (2004): 5964–5970.

9. D. A. Evans, D. M. Fitch, T. E. Smith, and V. J. Cee, "Application of Complex Aldol Reactions to the Total Synthesis of Phorboxazole B," *Journal of the American Chemical Society* 122 (2000): 10033–10046.

10. D. A. Evans, V. J. Cee, T. E. Smith, D. M. Fitch, and P. S. Cho, "Asymmetric Synthesis of Phorboxazole B—Part I: Synthesis of the C20-C38 and C39-C46 Subunits," *Angewandte Chemie, International Edition* 39 (2000): 2533–2536.

11. M. Moriyama, K. Nakata, T. Fujiwara, and Y. Tanabe, "Divergent Asymmetric Total Synthesis of All Four Pestalotin Diastereomers from (R)-Glycidol," *Molecules* 25 (2020): 394.

12. W. Dong, P. Hu, J. Hu, and X. Tong, "Lewis Base-Catalyzed Divergent Isomerizations of 5-Hydroxyl-2,3-Dienoate," *Tetrahedron Letters* 55 (2014): 1682–1685.

13. J. D. Winkler and K. Oh, "A One-Step Synthesis of 2,3-Dihydro-4-H-Pyran-4-Ones from 3-Ethoxy $\alpha,\beta$-Unsaturated Lactones," *Organic Letters* 7 (2005): 2421–2423.

14. I. Paterson, M. J. Coster, D. Y. K. Chen, K. R. Gibson, and D. J. Wallace, "The Stereocontrolled Total Synthesis of Altohyrtin A/Spongistatin 1: The CD-Spiroacetal Segment," *Organic & Biomolecular Chemistry* 3 (2005): 2410–2419.

15. S. J. Danishefsky and W. H. Pearson, "A New Strategy for the Synthesis of Spiroketals," *Journal of Organic Chemistry* 48 (1983): 3865–3866.

16. M. T. Crimmins and A. C. Smith, "A Hetero-Diels-Alder Approach to Complex Pyrones: An Improved Synthesis of the Spongistatin AB Spiroketal," *Organic Letters* 8 (2006): 1003–1006.

17. G. Peh and P. E. Floreancig, "Convergent One-Pot Oxidative [n + 1] Approaches to Spiroacetal Synthesis," *Organic Letters* 17 (2015): 3750–3753.

18. X. Han and P. E. Floreancig, "Spiroacetal Formation through Telescoped Cycloaddition and Carbon–Hydrogen Bond Functionalization: Total Synthesis of Bistramide A," *Angewandte Chemie, International Edition* 53 (2014): 11075–11078.

19. W. Szeja and G. Grynkiewicz, "Syntheses of Asymmetrically Substituted Pyrans of Natural Origin," in Natural Products as Source Molecules with Therapeutic Potential, ed. V. Cechinel Filho (Springer International Publishing, 2018), 233–307.

20. W. Zhi-Min and M. Shen, "An Efficient Synthesis of (−)-Pestalotin and Its Enantiomer Using Sharpless Asymmetric Dihydroxylation," *Tetrahedron: Asymmetry* 8 (1997): 3393–3396.

21. V. S. Mallula, B. Srinivas, and P. Radha Krishna, "Divergent Synthesis of (6S,1′S,2′R)-Hydroxypestalotin via Tandem Conjugate Addition–lactonization Sequence," *Tetrahedron Letters* 56 (2015): 1115–1117.

22. C. Donner, M. Gill, and L. Tewierik, "Synthesis of Pyran and Pyranone Natural Products," *Molecules* 9 (2004): 498–512.

23. N. P. H. Tan and C. D. Donner, "Total Synthesis and Confirmation of the Absolute Stereochemistry of Semiviriditoxin, a Naphthopyranone Metabolite from the Fungus Paecilomyces Variotii," *Tetrahedron* 65 (2009): 4007–4012.

24. S. Hanessian, T. Focken, and R. Oza, "Total Synthesis of Jerangolid A," *Organic Letters* 12 (2010): 3172–3175.

25. K. Mori, T. Otsuka, and M. Oda, "Synthesis of All of the Four Possible Stereoisomers of Pestalotin, a Gibberellin Synergist Isolated from Pestalotia Cryptomeriaecola Sawada," *Tetrahedron* 40 (1984): 2929–2934.

26. C. D. Donner, "Total Synthesis of (+)-Kalafungin Using a Tandem Michael–Dieckmann Approach," *Tetrahedron Letters* 48 (2007): 8888–8890.

27. U. Goergens and M. P. Schneider, "A Facile Enzyme Assisted Route to Enantiomerically Pure δ - Lactones," *Tetrahedron: Asymmetry* 3 (1992): 831–832.

28. M. Eskici, A. Karanfil, M. S. Özer, Y. Kabak, and İ. Durucasu, "Asymmetric Synthesis of ( *S*)-Dihydrokavain from l -Malic Acid," *Synthetic Communications* 48 (2018): 2382–2390.

29. R. Wethman, J. Derosa, V. T. Tran, et al., "An Under-Appreciated Source of Reproducibility Issues in Cross-Coupling: Solid-State Decomposition of Primary Sodium Alkoxides in Air," *ACS Catalysis* 11 (2021): 502–508.

30. For more details, See Supplementary Information.

31. D. B. G. Williams and M. Lawton, "Drying of Organic Solvents: Quantitative Evaluation of the Efficiency of Several Desiccants," *Journal of Organic Chemistry* 75 (2010): 8351–8354.

32. Alternatively, the formation of the intermediate *E*-**11a** anion via direct [1,5]-hydrogen transfer from adduct **10a** may be proposed, potentially facilitated by hydrogen bonding interactions with methanol or water.

33. P. Rivera-Quintero, G. S. Patience, N. A. Patience, D. C. Boffito, X. Banquy, and D. Schieppati, "Experimental Methods in Chemical Engineering: Karl Fischer Titration," *Canadian Journal of Chemical Engineering* 102 (2024): 2980–2997.

34. Deposition Numbers 2481003 (for *rac*-**1b**), 2481004 (for (*R*)-**1c**) contain the supplementary crystallographic data for this paper. These data are provided free of charge by the joint Cambridge Crystallographic Data Centre and Fachinformationszentrum Karlsruhe http://www.ccdc.cam.ac.uk/structures.


## Supporting Information

Additional supporting information can be found online in the Supporting Information section. The authors have cited additional references within the Supporting Information.[35–46] Reaction optimization data including the impact of the water contain and reaction workup on the reaction yields (Tables S1, S2, and S3; Scheme S2 and S3); detailed information on NMR experiments (Scheme S1; Figures S1 to S6); details about the computational study (Scheme S4); Experimental procedures and data characterization for all prepared compounds; A copy of $^{1}$H NMR and $^{13}$C{$^{1}$H} NMR spectra for all prepared compounds (PDF).